# Prediction and control of subsurface hooks in continuous cast ultra-low-carbon steel slabs

**G.-G. Lee*[1], H.-J. Shin[2], S.-H. Kim[1], S.-K. Kim[3], W.-Y. Choi[3] and B. G. Thomas[4]**

Subsurface hook formation during initial solidification in the continuous casting mould degrades the quality of steel slabs owing to the associated entrapment of argon bubbles and non-metallic inclusions. To minimise hook depth and to improve slab quality, extensive plant experiments were performed and analysed to quantify the effect of casting parameters on hook characteristics using the no. 2-1 caster at POSCO Gwangyang Works, Korea. The results reveal that meniscus heat flux plays an important role in controlling hook characteristics. Hook depth correlates with oscillation mark depth, hook shell thickness, and hook length. Based on regression analysis, this paper proposes an equation to predict hook depth in ultra-low-carbon steels as a function of casting speed, superheat, oscillation frequency, surface level fluctuations, and mould flux properties. Use of this quantitative equation enables improved control of subsurface quality in the continuous casting of steel slabs.

**Keywords:** Continuous casting, Subsurface quality, Hook, Solidification microstructure, Oscillation marks, Ultra low carbon steel

## Introduction

Periodic transverse depressions called 'oscillation marks' (OMs) are observed on the surface of steel slabs manufactured by continuous casting processes.[1–3] Hooks are another distinctive subsurface microstructural feature, and form at the meniscus during oscillation. They lead to surface defects such as slivers and blisters in the final rolled sheet product.[4,5] In extreme cases, the entire slab surface must be ground or 'scarfed' to remove all traces of the hook microstructure, resulting in higher cost and productivity loss.[6]

Many previous studies of slab quality have focused on the influences of operating parameters on OMs[4,5,7–11] and subsurface hooks.[12–16] Ultra-low-carbon (ULC) steel grades ($C \leqslant 0{\cdot}01$ wt%) are particularly prone to hook formation as shown in Fig. 1,[17,18] perhaps owing to higher liquidus temperature and thinner mushy zone[13] compared to other steel grades. These steels are designed for high ductility applications such as automobile exterior panels. Therefore, high surface slab quality is important in ULC steels. To minimise the depth of OMs and hooks and to increase slab quality, several different practices have been proposed and implemented in the industry. These include the use of mould powder with higher surface tension, higher viscosity and lower solidification temperature,[19] triangular mould oscillation,[20] changing the mould material for low thermal conductivity,[12] and applying electromagnetic fields for initial solidification control.[21,22]

Hooks and OMs form due to many interdependent, transient phenomena that occur simultaneously during initial solidification near the meniscus. Several different mechanisms have been proposed in previous literature. Sengupta *et al.*[23,24] have recently suggested a new mechanism for hook and OM formation, which is illustrated in Fig. 2. Hooks form in ULC steel by periodic meniscus solidification and subsequent liquid steel overflow and OMs form by normal steel shell growth before and after the overflow. This mechanism was based on a careful analysis of numerous specially etched samples from ULC steel slabs in controlled plant trials[6,25] at POSCO Gwangyang Works. Furthermore, this analysis explains observations in previous literature, theoretical modelling results,[23] and is supported by microstructural evidence obtained using[24] both optical microscopy and microanalysis techniques.

The present study was conducted to quantify the effect of casting conditions on OM and hook characteristics in ULC steels. Slab samples were collected during plant experiments at POSCO Gwangyang Works while controlling and measuring several operating parameters. Oscillation mark and hook characteristics were measured from sections of the slab samples and correlated with operating conditions. The results obtained from these different experiments suggest practical insights to decrease hooks and their associated surface defects by controlling the phenomena that cause them in the meniscus region for ULC steels.

[1]Department of Materials Science and Engineering, Pohang University of Science and Technology, Korea
[2]Steelmaking Research Group, POSCO Technical Research Laboratories, Korea
[3]Technology Development Group, POSCO Steelmaking Department, Gwangyang Works, Korea
[4]Department of Mechanical Science and Engineering, University of Illinois at Urbana-Champaign, USA

*Corresponding author, email yikoki@postech.ac.kr


Published by Maney on behalf of the Institute
Received 21 May 2008; accepted 1 July 2008
DOI 10.1179/174328108X369071

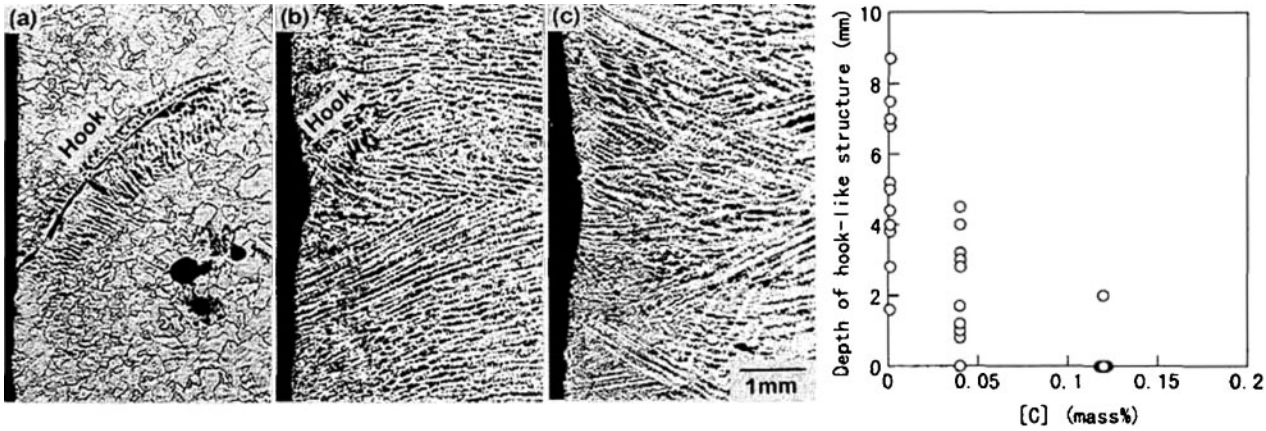


*a* 0·002%C; *b* 0·033%C; *c* 0·100%C

**1 Effect of steel carbon content on hook depth**

## Experimental

Four separate campaigns of plant experiments and laboratory analyses were performed from 2002 to 2005. Samples of ULC steel slabs were obtained from plant experiments performed on the no. 2-1 conventional vertical bending slab caster at POSCO Gwangyang Works, Korea, which features a conventional parallel mould with 230 mm thickness, standard two ports submerged entry nozzle (SEN), slide gate flow control with argon gas, non-sinusoidal hydraulic mould oscillator and electromagnetic brake ruler system. The composition of the ULC steel grade is given in Table 1.

During the 2002 tests, two plant trial sets were performed to investigate the effect of operating parameters on OM depth and hook characteristics. Test 1 was conducted at two different casting speeds with different slab width and electromagnetic current. Test 2 was conducted by changing mould oscillation conditions such as stroke, frequency, and modification ratio under the same casting speed, slab width and electromagnetic current.

From 2003 to 2005, plant experiments (Tests 3 and 4) were conducted with various casting speeds, slab widths, and electromagnetic currents using a different mould powder (Powder B) after performing Tests 1 and 2 (Powder A). In particular, Test 4 was performed to investigate the effect of casting speed on OM and hook formation. Details of the test conditions are given in Table 2 and the powder characteristics and properties are listed in Tables 3 and 4.

Samples ($230 \times 20 \times 100$ mm (width × depth × length) and encompassing ~10–12 OMs) were obtained near the surface of both narrow faces (NFs) of slabs for each test, as shown in Fig. 3. The left NF was analysed ultrasonically for entrapped particles (bubbles or/and inclusions) beneath the slab surface. The right NF was analysed metallographically to measure the OM and hook characteristics. Specifically, OM depth was

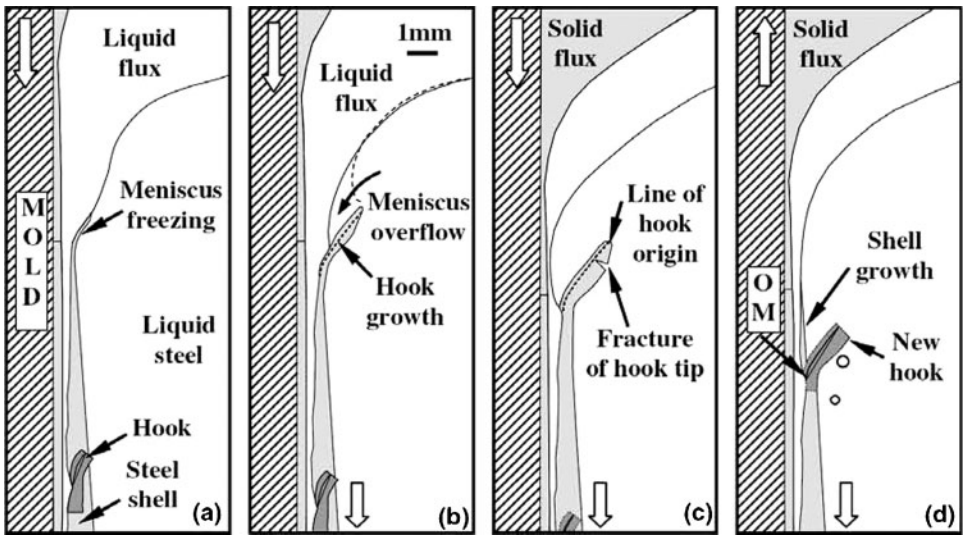


**2 Schematic illustrating formation of curved hooks in ULC steel slabs by meniscus solidification and subsequent liquid steel overflow[23,24]**

**Table 1 Composition of ULC steel tested, wt-% (Fe bal.)**

| C | Mn | Si | P | S | Cu | Ti | Al |
|---|---|---|---|---|---|---|---|
| 0·002–0·005 | 0·05–0·15 | ⩽0·005 | ⩽0·015 | ⩽0·010 | ~0·01 | ~0·050 | ~0·05 |

**Table 2 Test conditions from controlled plant experiments**

| Test no. | Slab width, mm | Casting speed, m min$^{-1}$ | Electromagnetic current, A | Tundish temperature, °C | Liquidus temperature, °C | Level fluctuation during sampling, mm | Oscillation stroke, mm | Oscillation frequency, cycle min$^{-1}$ | Non-sinusoidal mould oscillation ratio, % | Negative strip time, s | Positive strip time, s |
|---|---|---|---|---|---|---|---|---|---|---|---|
| Test 1-1 | 980 | 1·40 | 304·0 | 1559 | 1532·1 | 0·65 | 6·37 | 155 | 24 | 0·110 | 0·277 |
| Test 1-2 | 1050 | 1·70 | 405·0 | 1561 | 1532·1 | 1·05 | 6·82 | 181·3 | 24 | 0·095 | 0·236 |
| Test 2-1 | 1300 | 1·464 | 300·8 | 1566 | 1534·9 | 1·06 | 6·44 | 159·3 | 24 | 0·107 | 0·269 |
| Test 2-2 | 1300 | 1·457 | 300·6 | 1563 | 1534·9 | 1·78 | 5·00 | 145·7 | 0 | 0·115 | 0·296 |
| Test 2-3 | 1300 | 1·468 | 300·0 | 1571 | 1534·9 | 0·82 | 5·00 | 176·2 | 12 | 0·100 | 0·241 |
| Test 2-4 | 1300 | 1·496 | 297·4 | 1571 | 1534·2 | 0·94 | 5·00 | 209·4 | 24 | 0·081 | 0·205 |
| Test 2-5 | 1300 | 1·501 | 299·8 | 1555 | 1534·9 | 0·61 | 6·00 | 125·1 | 12 | 0·127 | 0·353 |
| Test 2-6 | 1300 | 1·468 | 300·2 | 1573 | 1534·2 | 0·65 | 6·00 | 146·8 | 24 | 0·110 | 0·299 |
| Test 2-7 | 1300 | 1·490 | 301·4 | 1566 | 1534·9 | 1·62 | 6·00 | 173·9 | 0 | 0·121 | 0·224 |
| Test 2-8 | 1300 | 1·487 | 302·0 | 1571 | 1534·9 | 0·96 | 7·00 | 106·2 | 24 | 0·139 | 0·426 |
| Test 2-9 | 1300 | 1·466 | 303·0 | 1559 | 1534·9 | 1·03 | 7·00 | 125·6 | 0 | 0·154 | 0·324 |
| Test 2-10 | 1300 | 1·493 | 300·4 | 1559 | 1534·9 | 0·76 | 7·00 | 149·3 | 12 | 0·126 | 0·276 |
| Test 3-1 | 1300 | 1·747 | 313·4 | 1560 | 1534·9 | 0·66 | 7·49 | 186·8 | 18 | 0·100 | 0·221 |
| Test 3-2 | 1300 | 1·418 | 234·2 | 1564 | 1535·0 | 0·47 | 6·84 | 154·7 | 18 | 0·118 | 0·269 |
| Test 3-3 | 1300 | 1·210 | 0·0 | 1564 | 1535·0 | 0·46 | 6·42 | 134·5 | 18 | 0·134 | 0·312 |
| Test 3-4 | 1300 | 1·474 | 277·0 | 1571 | 1535·0 | 0·71 | 6·95 | 160·2 | 18 | 0·115 | 0·260 |
| Test 3-5 | 1300 | 1·460 | 2·0 | 1567 | 1535·0 | 0·62 | 6·92 | 158·9 | 18 | 0·116 | 0·262 |
| Test 4-1 | 950 | 1·803 | 456·8 | 1559 | 1533·5 | 0·54 | 6·30 | 192·3 | 19 | 0·092 | 0·220 |
| Test 4-2 | 950 | 1·805 | 457·0 | 1559 | 1533·5 | 0·37 | 6·30 | 192·4 | 19 | 0·092 | 0·220 |
| Test 4-3 | 950 | 1·793 | 307·6 | 1559 | 1533·5 | 0·12 | 6·29 | 191·3 | 19 | 0·092 | 0·221 |
| Test 4-4 | 1300 | 1·692 | 232·0 | 1564 | 1534·9 | 1·99 | 6·19 | 181·5 | 19 | 0·092 | 0·234 |
| Test 4-5 | 1300 | 1·396 | 232·2 | 1564 | 1534·9 | 0·72 | 5·90 | 152·6 | 19 | 0·114 | 0·279 |
| Test 4-6 | 1300 | 1·684 | 232·2 | 1565 | 1534·9 | 0·94 | 6·18 | 180·7 | 19 | 0·097 | 0·235 |
| Test 4-7 | 1300 | 1·689 | 235·8 | 1564 | 1534·9 | 0·62 | 6·19 | 181·2 | 19 | 0·097 | 0·234 |
| Test 4-8 | 1440 | 1·506 | 190·4 | 1562 | 1534·9 | 0·55 | 6·01 | 163·4 | 19 | 0·107 | 0·261 |
| Test 4-9 | 1440 | 1·509 | 236·0 | 1562 | 1534·9 | 1·36 | 6·01 | 163·6 | 19 | 0·107 | 0·260 |
| Test 4-10 | 1570 | 1·373 | 139·8 | 1566 | 1534·6 | 0·80 | 5·87 | 150·4 | 19 | 0·115 | 0·284 |
| Test 4-11 | 1570 | 1·374 | 140·0 | 1565 | 1534·2 | 1·28 | 5·87 | 150·5 | 19 | 0·115 | 0·283 |
| Test 4-12 | 1570 | 0·990 | 0·0 | 1568 | 1534·2 | 3·07 | 5·49 | 113·0 | 19 | 0·152 | 0·379 |
| Test 4-13 | 1570 | 0·835 | 0·0 | 1570 | 1534·2 | 1·45 | 5·34 | 97·9 | 19 | 0·175 | 0·438 |

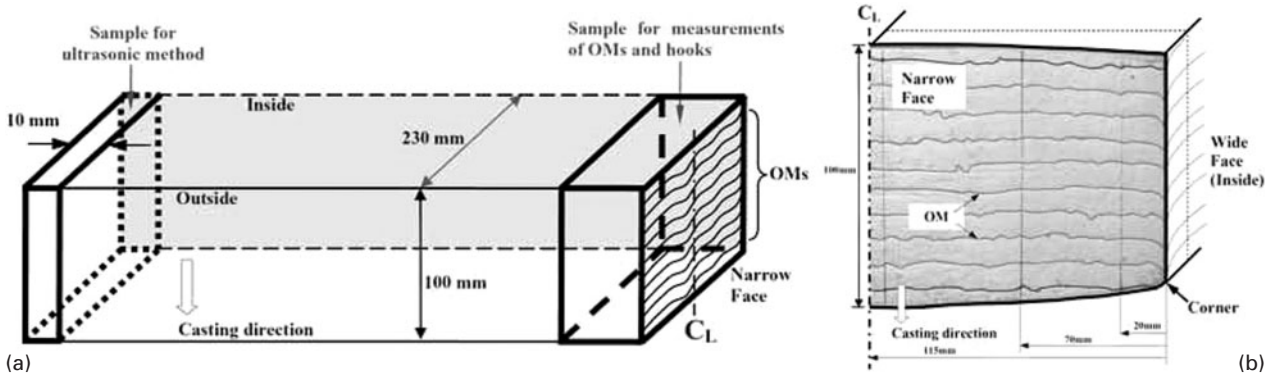


**3 Schematic showing sample locations for *a* both NFs and *b* measurements of OMs and hooks on right NF**

measured along an 80 mm length of right NF using a laser based profilometer along 21 different lines down the NF surface. Hook characteristics were measured at five different distances between the wide faces (WFs). Further WF slab samples were taken from Test 4 conditions, and hook depths were measured from 1/4 position from the corner. Sections through each sample were cut, ground, polished to $\sim$0·25 μm and then etched by a special etching method[24] for ULC steel to reveal the microstructure and hook shapes.

## Results and discussion

### Hook characteristics definitions

Hook characteristics include depth, length, angle, and shell thickness as illustrated in Fig. 4. The hook depth is defined for this study as the perpendicular distance from the slab surface to furthest inner extent of the hook, because this indicates the thickness of surface layer that should be removed during scarfing process to completely eliminate hooks and their associated surface defects. Hook length is defined as the linear distance from the starting point of the line of hook origin near the OM to its end point. Hook angle is derived from the depth and length and indicates how much the hook bends away from the slab surface. Hook shell thickness is usually measured at the upper end of the OM where the hook starts, which generally represents the thicker part of the hook. The OM depth is the perpendicular distance from the deepest point of the OM valley to the reasonably flat slab surface. The average OM and hook characteristics obtained from slab samples of the right NF are given in Table 5.

In addition, the compositions of subsurface defects observed in optical micrographs near the hook region were analysed by energy dispersive X-ray spectroscopy, as shown in Fig. 5. The complex oxides suggest mould flux and the round bubble shows evidence of non-metallic inclusions attached to it. These results show that both non-metallic inclusions and bubbles can be entrapped on the front of the solidifying shell, or hook during initial solidification at the meniscus. This agrees with previous findings.[4,18]

### Oscillation marks depth correlation with hook shape

Results in Fig. 6 show that deeper hooks are accompanied by deeper OMs. Thus, OM depth can be used as an approximate indicator of hook depth and slab surface quality without metallographic analysis of the slabs. Many casting conditions were varied during the plant experiments, such as casting speed, slab width, mould powder, superheat, fluid flow conditions, and oscillating practice, etc. The effects of these important casting variables will be discussed in the following sections.

### Hook shell thickness correlation with hook depth

Figure 7 shows that hook depth is linearly proportional to hook shell thickness. This trend holds strongly even if conditions such as mould oscillation practice have been severely changed (Test 2). This finding is consistent with the hook formation mechanism in Fig. 2, which involves meniscus freezing and subsequent liquid steel overflow suggested by Sengupta *et al.*[23] Based on this mechanism, increasing the hook shell thickness indicates that either

**Table 3 Mould powder compositions, wt-%**

| | Basicity | $SiO_2$ | CaO | MgO | $Al_2O_3$ | $TiO_2$ | $Fe_2O_3$ | $MnO_2$ | $P_2O_5$ | $Na_2O$ | $K_2O$ | F | $B_2O_3$ | $Li_2O$ |
|---|---|---|---|---|---|---|---|---|---|---|---|---|---|---|
| Powder A (Tests 1 and 2) | 1·1 | 36·33 | 39·80 | 0·84 | 5·97 | 0·18 | 0·34 | 0·03 | 0·03 | 3·43 | 0·11 | 6·72 | 0·0 | 0·35 |
| Powder B (Tests 3 and 4) | 1·0 | 37·77 | 37·88 | 1·98 | 4·99 | 0·03 | 0·31 | 0·04 | 0·01 | 3·75 | 0·11 | 7·22 | 1·20 | 0·90 |

**Table 4 Mould powder properties**

| | Bulk density, g $mL^{-1}$ | Solidification temperature, °C | Softening temperature, °C | Melting temperature, °C | Viscosity (poise) at 1300°C |
|---|---|---|---|---|---|
| Powder A (Tests 1 and 2) | 0·82 | 1150 | 1170 | 1180 | 3·21 |
| Powder B (Tests 3 and 4) | 0·85 | 1100 | 1150 | 1150 | 2·62 |

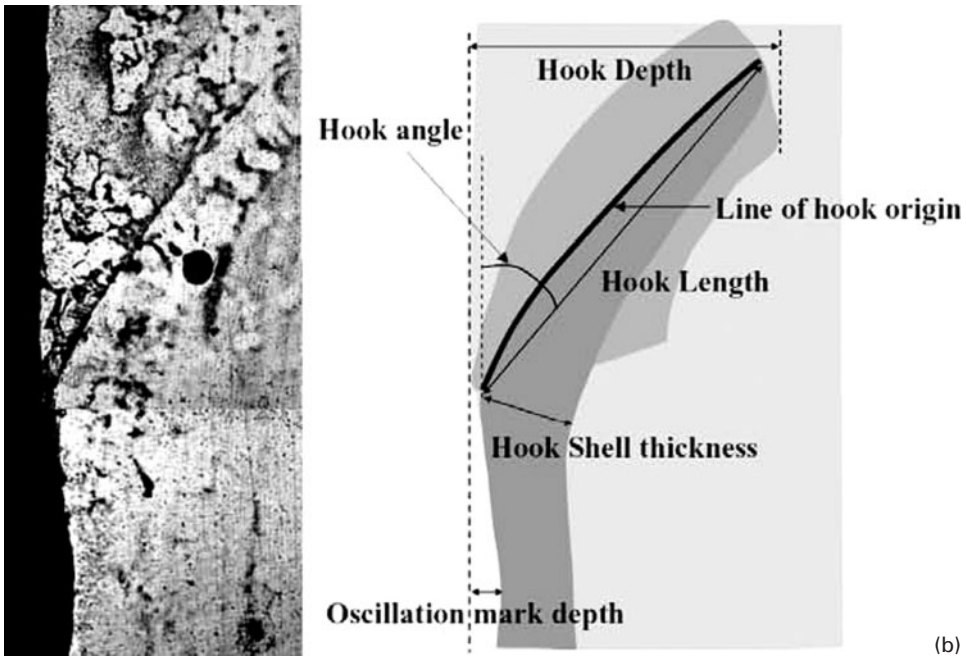


**4** ***a*** **typical shape of curved hook with entrapped bubble and** ***b*** **definitions of hook characteristics**

the time for the hook growth was longer or the extent of undercooling during liquid steel overflow was more pronounced. In either case, meniscus freezing is promoted so the hook becomes both thicker and longer.

## Superheat effects

The effect of superheat temperature difference on hook characteristics was evaluated as part of Test 2. The superheat in this study is based on tundish temperature, which should correlate with superheat at the meniscus, if the mould flow pattern stays constant. The hook length decreases dramatically for superheats above 30°C, as shown in Fig. 8. A thinner hook shell can be expected if the solidification time at the meniscus is shorter (*see* previous section), or if the superheat delivery is higher. Although the study in Fig. 9 was conducted to

**Table 5 Mean value of hook characteristics and OM depth**

| Test no. | Measured hook depth, mm | Measured hook l ength, mm | Measured hook angle, ° | Measured hook shell thickness, mm | Measured OM depth, mm |
|---|---|---|---|---|---|
| Test 1-1 | 1·87 | 6·37 | 18·5 | – | 0·440 |
| Test 1-2 | 1·2 | 2·81 | 30·0 | – | 0·286 |
| Test 2-1 | 1·68 | 2·16 | 34·3 | 0·71 | 0·246 |
| Test 2-2 | 2·16 | 4·72 | 19·8 | 0·86 | 0·393 |
| Test 2-3 | 1·39 | 2·16 | 27·6 | 0·66 | 0·309 |
| Test 2-4 | 1·54 | 2·41 | 29·7 | 0·65 | 0·292 |
| Test 2-5 | 1·72 | 3·34 | 23·1 | 0·76 | 0·353 |
| Test 2-6 | 1·69 | 2·75 | 28·7 | 0·7 | 0·343 |
| Test 2-7 | 1·59 | 2·77 | 27·5 | 0·62 | 0·258 |
| Test 2-8 | 1·89 | 3·08 | 29·7 | 0·78 | 0·308 |
| Test 2-9 | 2·32 | 4·87 | 21·6 | 0·92 | 0·338 |
| Test 2-10 | 1·94 | 4·58 | 20·2 | 0·78 | 0·331 |
| Test 3-1 | 1·1 | 2·0 | 27·0 | 0·46 | 0·251 |
| Test 3-2 | 1·22 | 1·77 | 30·9 | 0·52 | 0·328 |
| Test 3-3 | 1·3 | 1·63 | 34·6 | 0·60 | 0·280 |
| Test 3-4 | 1·18 | 1·83 | 26·1 | 0·56 | 0·313 |
| Test 3-5 | 1·06 | 1·65 | 28·0 | 0·46 | 0·272 |
| Test 4-1 | 0·83 | – | – | 0·45 | 0·225 |
| Test 4-2 | 0·83 | – | – | 0·41 | 0·214 |
| Test 4-3 | 0·73 | – | – | 0·38 | 0·199 |
| Test 4-4 | 0·77 | – | – | 0·47 | 0·192 |
| Test 4-5 | 1·11 | – | – | 0·51 | 0·302 |
| Test 4-6 | 1·06 | – | – | 0·53 | 0·236 |
| Test 4-7 | 0·96 | – | – | 0·47 | 0·277 |
| Test 4-8 | 1·09 | – | – | 0·49 | – |
| Test 4-9 | 1·03 | – | – | 0·46 | – |
| Test 4-10 | 1·12 | – | – | 0·57 | 0·310 |
| Test 4-11 | 1·05 | – | – | 0·53 | 0·304 |
| Test 4-12 | 1·79 | – | – | 0·73 | 0·495 |
| Test 4-13 | 1·62 | – | – | 0·71 | 0·566 |

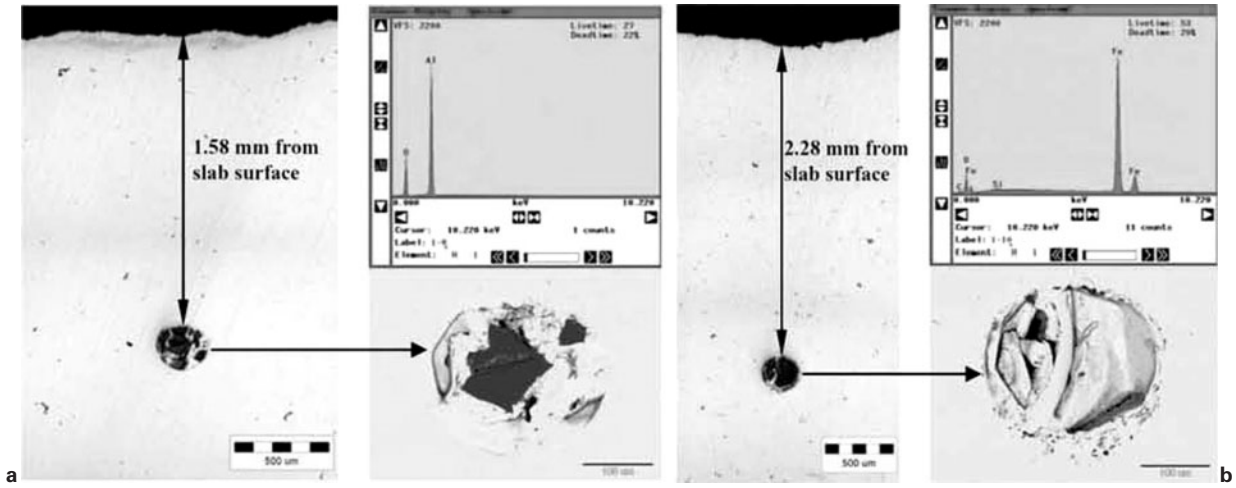


5 Optical micrographs showing entrapment of inclusions attached to round bubble beneath slab surface

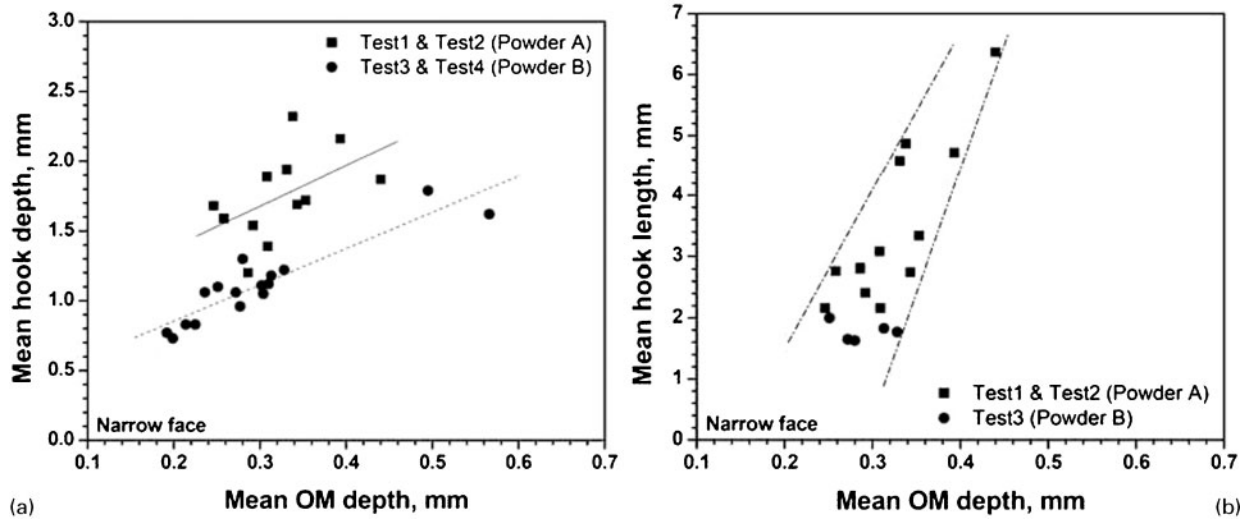


6 Relation between OM depth and hook shape: *a* depth and *b* length

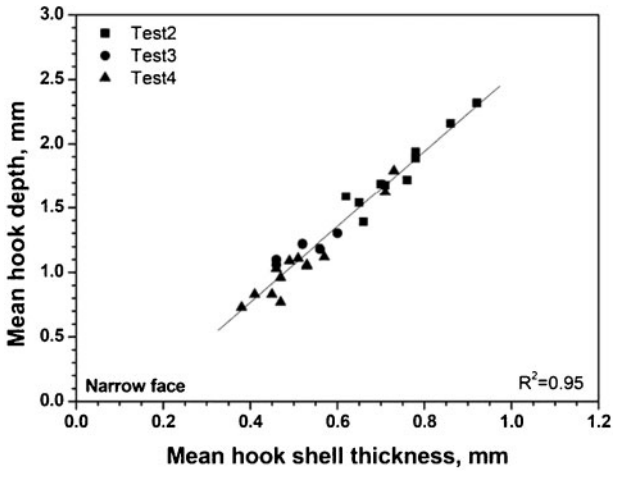


7 Relation between hook shell thickness and depth

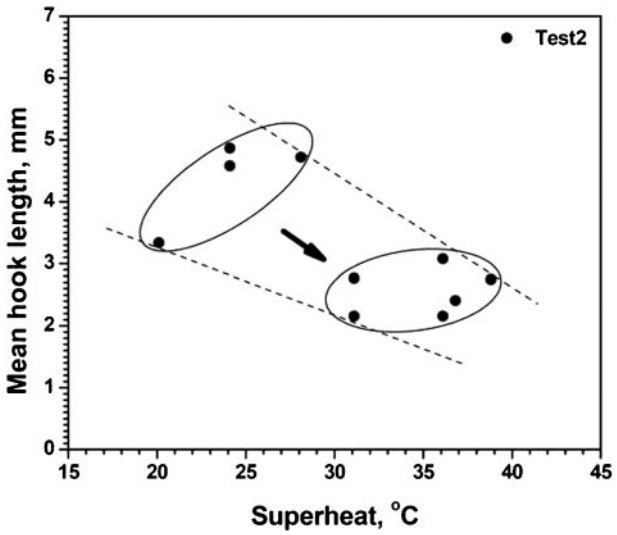


8 Effect of superheat in tundish on hook length

investigate frequency, the effect of superheat was so important that the results were divided up accordingly. Figure 9*a* shows that the higher superheats produce thinner hooks. Figure 9*b* shows that higher superheat produces both shorter hooks and thinner hooks. Higher superheat delivery tends to make thinner and shallower hooks. Moreover, previous works have shown that hooks near the slab corners are deeper than other regions along the mould perimeter, owing to the lower superheat, and ease of meniscus overflow there.[26] These

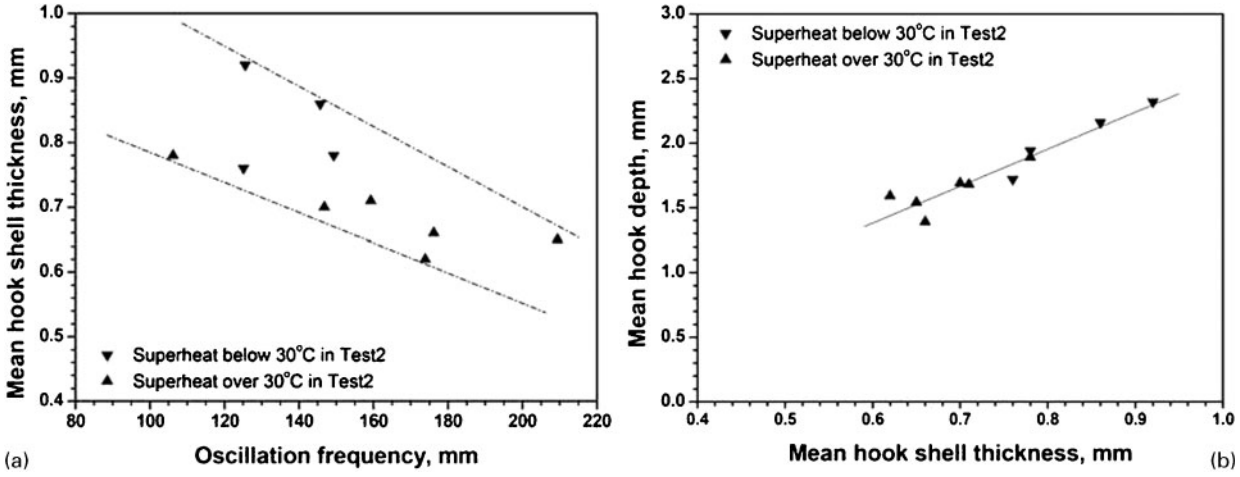


**9 Relation between superheat and hook shape**

results show that raising superheat is one of the most important methods to minimise hook formation during initial solidification.

## Casting speed effects

To investigate the effect of casting speed on both OM and hook depths, two different sets of plant experiments were performed between 2002 and 2005. First, three casting speeds (1·40, 1·45 and 1·70 m min$^{-1}$) are considered with different slab width in Tests 1 and 2-1. Figure 10 shows optical micrographs of subsurface hooks obtained from specially etched samples at different casting speeds. Figure 11 shows the number of entrapped particles (bubbles and/or inclusions) per unit area in samples from the left NF slab, as shown in Fig. 3*a*. Increasing casting speed shows a marked decrease in surface defects, contrary to expectations related to surface level fluctuation effects. These results suggest that the higher superheat found at higher casting speed is responsible for lowering hook depth and their associated surface defects.

Another set of plant experiments (Tests 3 and 4) involved more systematic measurements to quantify the effect of various casting speeds and slab widths on both OM and hook depths. First, increasing casting speed is known to cause a significant increase in heat extraction at the meniscus region,[27] resulting in higher heat flux, as shown in Fig. 12. Mean heat flux is defined as the total heat removed by the cooling water per unit area of strand surface, which is based on the measured temperature difference of the cooling water between inlet and outlet. Increasing meniscus heat flux would be expected to make hooks more severe. However, Huang and Thomas[28] noted the opposing effect that increasing the casting speed increases the local superheat delivered at the solidification front, so discourages meniscus freezing. This latter effect seems to be more important, according to the results in Figs. 13 and 14 of the current work.

Figure 13 shows that both OM and hook depths are clearly decreased with increasing casting speed, as a function of oscillation conditions such as stroke and frequency. For this analysis, nine oscillation tests (Tests 2-2 to 2-10) were excluded from these results because casting speed was not dependent on oscillation conditions. In addition, hook depth on the WF at 1/4 position from the corner was examined with different casting speed, as shown in Fig. 14. These results again confirm that OM and hook depths decrease with increasing casting speed and the trend of decreasing hook depth with casting speed agrees with the results measured by Awajiya *et al.*[29] Hence, increasing casting speed, which increases flowrate of molten steel from the SEN, is expected to carry more heat to retard the initial solidification at the meniscus.

In summary, the results from several sets of tests conducted over several years show that increasing casting speed helps to increase heat delivery to the meniscus and to minimise hook and OM depths and their accompanying surface defects.

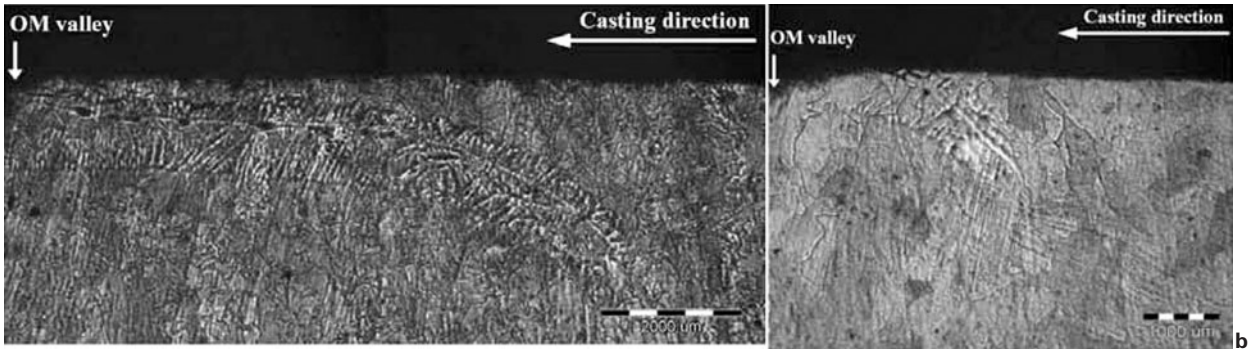


a b

*a* 1·40 m min$^{-1}$; *b* 1·70 m min$^{-1}$

**10 Optical micrographs of subsurface hook at different casting speeds**

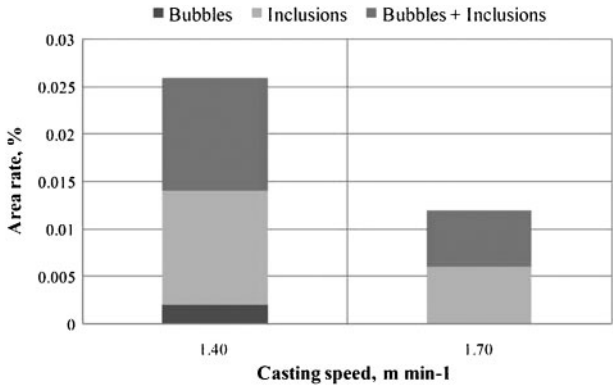


**11 Relation between casting speed and surface defects**

## Mould powder effects

Figures 6 and 13 also show that powder properties greatly affect OM and hook depths. In this case, Powder B with a lower solidification temperature and viscosity produces significantly less OM and hook depths. This effect agrees with Bommaraju *et al.*[19] who have reported that mould powder with a lower solidification temperature, has shallower OM depth. This might be due to smaller slag rim solidified on the mould wall. The lower viscosity of the mould powder allows easier steel overflow at the meniscus after it freezes during hook formation. This agrees with the mechanism which was proposed by Hill *et al.*[30] but not with that of Kobayashi and Maruhashi.[31] Thus optimising mould powder properties is one of the most important parameters for controlling hook depth.

## Level fluctuation effects

It is well known from previous work that level fluctuations are detrimental to surface quality.[32,33] In the current work, OM and hook depths roughly appear to decrease with decreasing level fluctuation during sampling, as shown in Fig. 15. The weakness of this trend may be due to the difference of position between meniscus region and level sensor, and level fluctuations were recorded once per second using the continuous caster monitoring system, relative to about four mould oscillations per second. Sengupta *et al.* and Zhu[34,35]

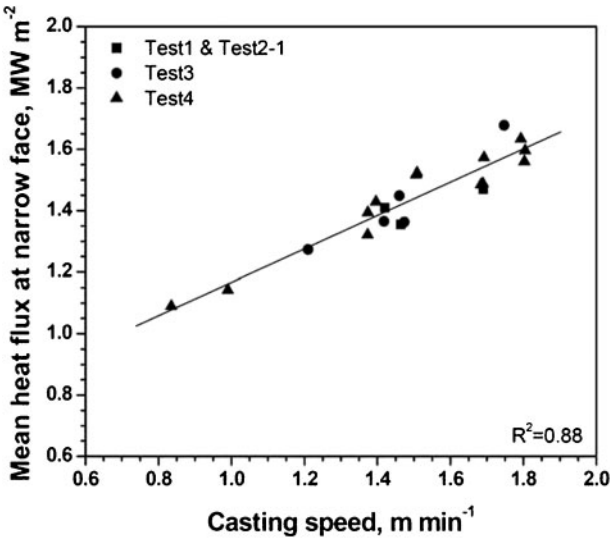


**12 Relation between casting speed and heat flux at NF**

have suggested that the thermal distortion due to a sudden level fluctuation event can cause:

(i) the shell tip to bend away from the mould due to sudden level drop
(ii) the shell tip to further bend during the subsequent rise in liquid level.

This is especially important for the shallower straight hooks. Larger level fluctuations generate deeper OMs and hooks, and also exacerbate the capture of mould slag at the solidification front. Larger level fluctuations also accompany faster, hotter steel flow to the meniscus, which is beneficial, and may explain the scatter in the trend. These results confirm the importance of controlling other casting conditions such as fluid flow in the mould, to control hook formation.

## Mould oscillation condition effects

To investigate the effect of oscillation conditions on both OMs and hooks characteristics, Test 2 plant experiments were performed holding other conditions constant, including the casting speed, slab width, mould powder (Powder A), and electromagnetic current. Figure 16 shows the effect of oscillation conditions on OM and hook depths from Test 2. Hook depth appears

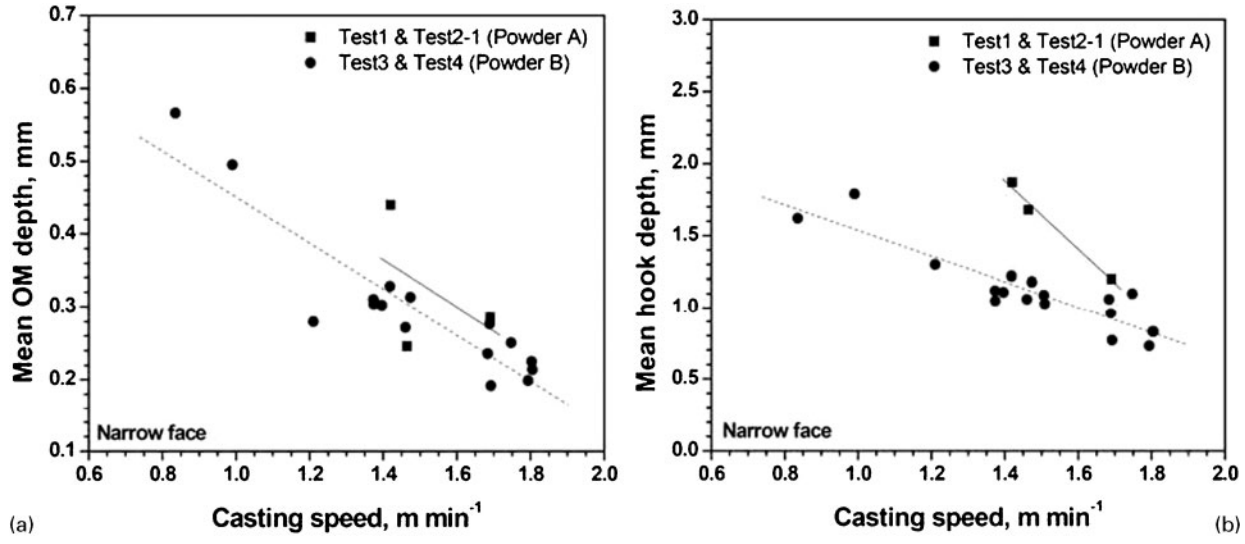


**13 Effect of casting speed on *a* OM and *b* hook depths on NF**

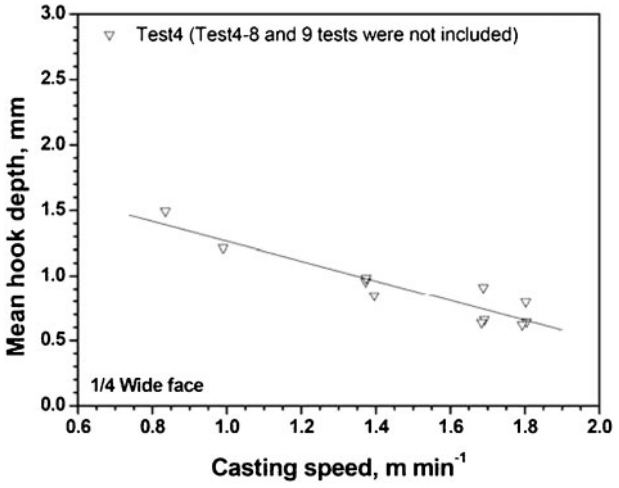


14 **Effect of casting speed on hook depth of WF**

to decrease with increasing oscillation frequency, but the trend with OM depth is very rough. It is difficult, however, to find a trend with stroke. Positive strip time decreases with increasing oscillation frequency, so increasing frequency shortens the solidification time. This effect helps to explain how higher frequency can produce shallower OM and hook depths with better slab surface quality. The roughness of these trends suggests that oscillation parameters are less important than the other casting conditions discussed in the previous sections.

The effects of negative and positive strip time are shown in Fig. 17, divided into two groups of higher and lower superheat in Test 2 plant experiments. The hook depth roughly decreases with decreasing negative strip time or decreasing positive strip time, at least for higher superheats. The importance of the superheat effect helps to explain the roughness in the trends.

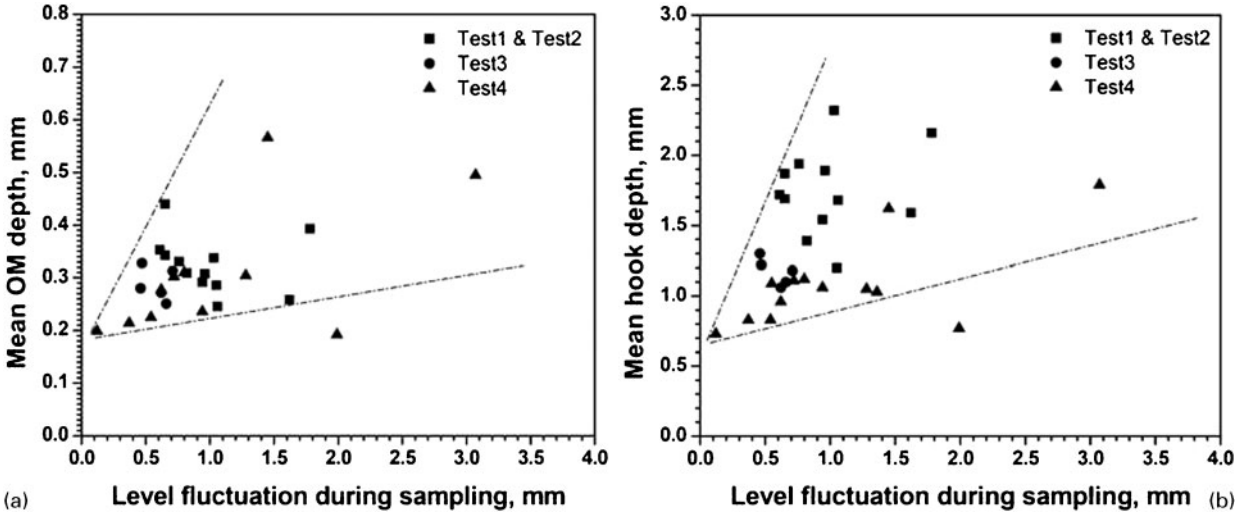


15 **Effect of level fluctuation during sampling on *a* OM and *b* hook depths**

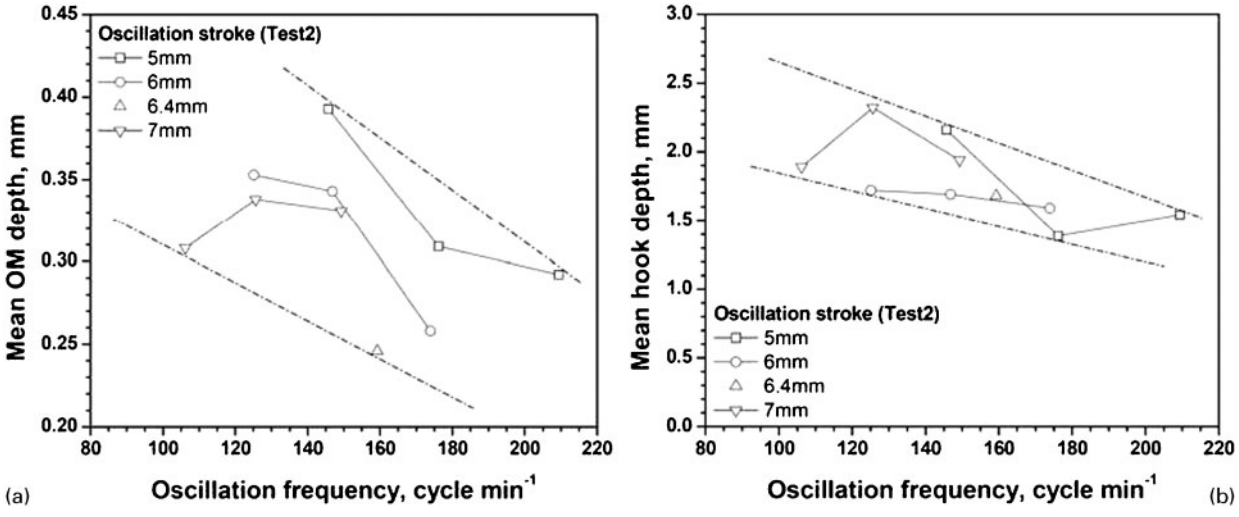


16 **Effect of oscillation frequency on *a* OM and *b* hook depths**

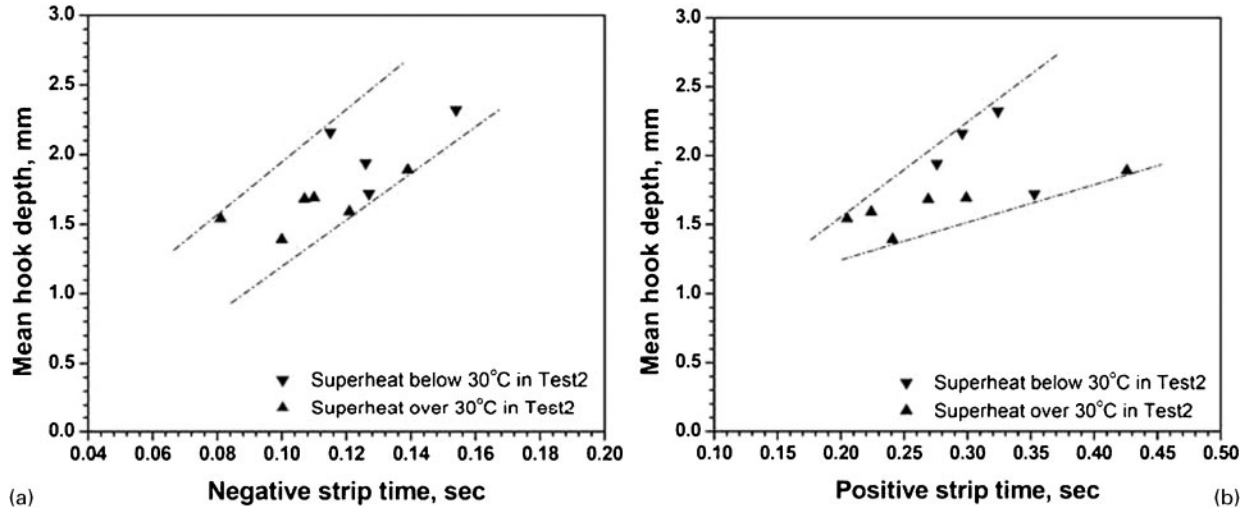


*a* negative strip time; *b* positive strip time

**17 Effect of mould oscillation on hook depth**

## Empirical equation for hook depth

From regression of the results, the following empirical equation was derived to predict the average hook depth in ULC steel slabs from the casting conditions

$$\text{Predicted hook depth} = 10^{-31.0874} \times V_c^{-0.61416} \times F^{-0.46481} \times T_S^{-0.18782} \times L_F^{0.041863} \times T_{sol}^{10.692}$$

where $V_c$ is the casting speed (m min$^{-1}$), $F$ is the oscillation frequency (cycle min$^{-1}$), $T_S$ is the superheat temperature difference (°C) defined as ($T_{tundish} - T_{liquidus}$), $L_F$ is the mean level fluctuation during sampling (mm) and $T_{sol}$ is the solidification temperature of mould powder. Figure 18 compares measured hook depths with predictions using this equation.

## Conclusion

This study presents the results of extensive parametric plant measurements of continuous cast steel slabs to quantify the effect of process conditions on OM depth and hook characteristics. Shallower hooks correlate with shorter hooks, thinner hooks, and shallower OM depth. Hooks and their associated surface defects can be decreased by controlling the phenomena that cause them. Increasing superheat delivery to the meniscus region with increasing casting speed has a strong effect on decreasing OM and hook depths. Optimising of mould powder properties can greatly affect hook characteristics. Level fluctuations affect hook depth. Control of casting conditions related to heat flux near the meniscus region is the key to decreasing hook depth and increasing slab quality by optimising process conditions.

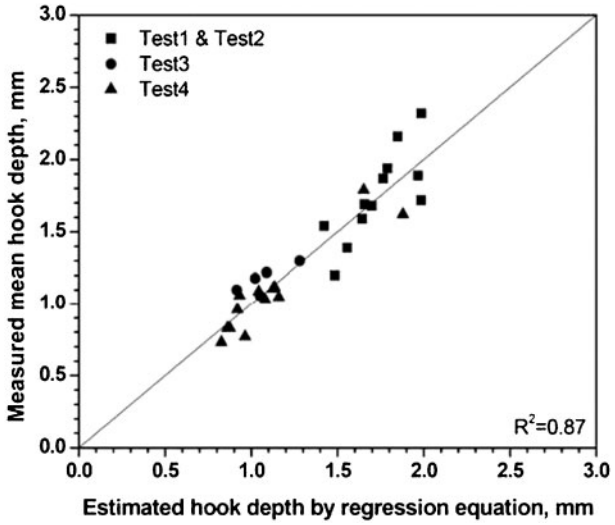


**18 Simple empirical equation with experimental results**

## Acknowledgement

The authors thank the continuous casting team in Technology Development Groups of Steelmaking Department at POSCO Gwangyang Works for their efforts and cooperation during plant experiments and the Continuous Casting Consortium, the University of Illinois at Urbana-Champaign for support of this project.

## References

1. E. Takeuchi and J. K. Brimacombe: *Metall. Trans. B*, 1985, **16B**, 605–625.
2. E. Takeuchi and J. K. Brimacombe: *Metall. Trans. B*, 1984, **15B**, 493–509.
3. J. K. Brimacombe and K. Sorimachi: *Metall. Trans. B*, 1977, **8B**, 489–505.
4. J.-P. Birat, M. Larrecq, J.-Y. Lamant, J. Petegnief and K. T. Muller: Steelmaking Conf. Proc., Warrendale, PA, USA, April 1991, Iron and Steel Society, Vol. 74, 39–50.
5. T. Emi, H. Nakato, Y. Iida, K. Emoto, R. Tachibana, T. Imai and H. Bana: Proc. Nat. Open Hearth and Basic Oxygen Steel Conf., Chicago, IL, USA, Vol. 61, 350–361; 1978, Warrendale, PA, ISS.
6. H.-J. Shin, B. G. Thomas, G.-G. Lee, J.-M. Park, C.-H. Lee and S.-H. Kim: MS&T 2004 Conf. Proc., 11–26; 2004, New Orleans, LA, AIST.
7. M. M. Wolf: Steelmaking Conf. Proc., Vol. 74, 51–71; 1991, Warrendale, PA, ISS.
8. R. V. Mahapatra, J. K. Brimacombe and I. V. Samarasekera: *Metall. Trans. B*, 1991, **22B**, 875–888.
9. S. Harada, S. Tanaka, H. Misumi, S. Mizoguchi and J. Horiguchi: *ISIJ Int.*, 1990, **30**, 310–316.
10. A. W. Cramb and F. J. Mannion: Steelmaking Conf. Proc., Vol. 68, 349–359; 1985, Warrendale, PA, ISS.
11. H. Nakato, S. Matsumura, Y. Habu, H. Oka and T. Ueda: *Tetsu-to-Hagane*, 1983, **69**, 248–253.
12. A. Yamauchi, S. Itoyama, Y. Kishimoto and T. Watanabe: *ISIJ Int.*, 2002, **42**, 1094–1102.

13. H. Yamamura, Y. Mizukami and K. Misawa: *ISIJ Int.*, 1996, (Suppl.), S223–226.
14. M. M. Wolf: in 'Solidification processing 1987', 182–186; 1987, Sheffield, The Institute of Metals.
15. H. Nakato, T. Nozaki, Y. Habu, H. Oka, T. Ueda, Y. Kitano and T. Koshikawa: Steelmaking Conf. Proc., Vol. 68, 361–365; 1985, Warrendale, PA, ISS.
16. M. M. Wolf and W. Kurz: in 'Solidification and casting of metals', 287–294; 1977, Sheffield, The Metals Society.
17. M. Suzuki: *CAMP-ISIJ*, 1998, **11**, 42–44.
18. Y. Kitano, K. Kariya, R. Asaho, A. Yamauchi and S. Itoyama: *Testsu-to-Hagane*, 1994, **80**, T165–168.
19. R. Bommaraju, T. Jackson, J. Lucas, G. Skoczylas and B. Clark: *Iron Steelmaker*, 1992, **19**, 21–27.
20. J.-P. Birat: *Revue de Metallurgie-CIT*, 1982, **79**, 603–616.
21. M. Tani, T. Toh, H. Harada, K. Fujisaki, E. Anzai and T. Matsumiya: *CAMP-ISIJ*, 2002, **15**, 831–834.
22. T. Tho, E. Takeuchi, M. Hojo, H. Kawai and S. Matsumura: *ISIJ Int.*, 1997, **37**, 1112–1119.
23. J. Sengupta, B. G. Thomas, H. J. Shin, G. G. Lee and S. H. Kim: *Metall. Mater. Trans. A*, 2006, **37A**, 1597–1611.
24. J. Sengupta, H.-J. Shin, B. G. Thomas and S. H. Kim: *Acta Mater.*, 2006, **54**, 1165–1173.
25. H.-J. Shin, G.-G. Lee, W.-Y. Choi, S.-M. Kang, J.-H. Park, S.-H. Kim and B. G. Thomas: Proc. Conf. AISTech 2004, Nashvillle, TN, USA, September 2004, the Association for Iron and Steel Technology, Vol. 1, 56–69.
26. G. G. Lee, B. G. Thomas, S. H. Kim, H. J. Shin, S. K. Baek, C. H. Choi, D. S. Kim and S. J. Yu: *Acta Mater.*, 2007, **55**, 6705–6712.
27. R. B. Mahapatra, J. K. Brimacombe and I. V. Samarasekera: *Metall. Trans. B*, 1991, **22B**, 875–888.
28. X. Huang and B. G. Thomas: *Can. Metall. Q.*, 1998, **37**, 197–212.
29. Y. Awajiya, J. Kubota and S. Takeuchi: Proc. Conf. AISTech 2005, Charlotte, NC, USA, May 2005, the Association for Iron and Steel Technology, Vol. 2, 65–74.
30. J. M. Hill, Y. H. Wu and B. Wiwatanapataphee: *J. Eng. Math.*, 1999, **36**, 311–326.
31. Y. Kobayashi and S. Maruhashi: 4th Japan-CSSR Semin., Ostrava, Czechoslovakia, 1983; 249.
32. J. Kubota, K. Okimoto, M. Suzuki, A. Shirayama and T. Masaoka: Proc. 6th Int. Iron Steel Cong., Nagoya, Japan, October 1990, ISIJ, Vol. 3, 356–363.
33. Y. Sasabe, S. Kubota, A. Koyama and H. Miki: *ISIJ*, 1990, **30**, 136–141.
34. B. G. Thomas and H. Zhu: JIM/TMS Solidification Sci. Process. Conf., Honolulu, HI, December 1995, JIM/TMS, 197–208.
35. J. Sengupta and B. G. Thomas: Proc. 11th Int. Conf. on 'Modeling of casting, welding and advanced solidification processes', Opio, France, May–June 2006, TMS, 727–236.